

# Tidal disruptions of separated binaries in galactic nuclei

Pau Amaro-Seoane,<sup>1,2\*</sup> M. Coleman Miller<sup>3</sup> and Gareth F. Kennedy<sup>4</sup>

<sup>1</sup>Max Planck Institut für Gravitationsphysik (Albert-Einstein-Institut), D-14476 Potsdam, Germany

<sup>2</sup>Institut de Ciències de l'Espai (CSIC-IEEC), Campus UAB, Torre C-5, parells, 2<sup>nd</sup> planta, ES-08193, Bellaterra, Barcelona, Spain

<sup>3</sup>Department of Astronomy and Joint Space-Science Institute, University of Maryland, College Park, MD 20742-2421, USA

<sup>4</sup>Institut de Ciències del Cosmos, Facultat de Física Martí i Franquès, 1 E-08028 Barcelona, Spain

Accepted 2012 April 23. Received 2012 April 19; in original form 2011 May 27

## ABSTRACT

Several galaxies have exhibited X-ray flares that are consistent with the tidal disruption of a star by a central supermassive black hole. In theoretical treatments of this process it is usually assumed that the star was initially on a nearly parabolic orbit relative to the black hole. Such an assumption leads in the simplest approximation to a  $t^{-5/3}$  decay of the bolometric luminosity and this is indeed consistent with the relatively poorly sampled light curves of such flares. We point out that there is another regime in which the decay would be different: if a binary is tidally separated and the star that remains close to the hole is eventually tidally disrupted from a moderate eccentricity orbit, the decay is slower, typically  $\sim t^{-1.2}$ . As a result, careful sampling of the light curves of such flares could distinguish between these processes and yield insight into the dynamics of binaries as well as single stars in galactic centres. We explore this process using three-body simulations and analytic treatments and discuss the consequences for present-day X-ray detections and future gravitational wave observations.

**Key words:** black hole physics – gravitational waves – hydrodynamics – X-rays: general.

## 1 INTRODUCTION

In the past few years, several galaxies have exhibited X-ray/ultraviolet flares consistent with the tidal disruption of a star by a supermassive black hole (SMBH; for flare observations see Donley et al. 2002; Dogiel et al. 2009; Gezari et al. 2009). These candidate disruptions are relevant to the fuelling of some active galactic nuclei (AGN; particularly low-mass ones; see Wang & Merritt 2004) and contain important information about stellar dynamics in the centres of galaxies. In addition, they are related to one of the processes believed to lead to extreme mass ratio inspirals (EMRIs), in which a stellar-mass object spirals into an SMBH; EMRIs are thought to be among the most promising sources for milli-Hertz gravitational wave detectors such as the evolved *Laser Interferometer Space Antenna* (LISA; see Amaro-Seoane et al. 2007, 2012).

Analyses of stellar tidal disruptions have focused on stars whose orbits are nearly parabolic relative to the SMBH (Rees 1988). In this case, roughly half of the stellar material becomes unbound and the rest rains down on the SMBH with a rate that, for simplified stellar structure, scales with the time  $t$  since disruption as  $\dot{M} \sim t^{-5/3}$  (this is expected at late times even for more realistic structure; see Lodato, King & Pringle 2009).

There is, however, another possible path to disruptions. Binaries that get close enough to an SMBH can be tidally separated without destroying either star. The result is that one star becomes relatively tightly bound to the SMBH whereas the other is flung out at high speed. The bound star will undergo dynamical interactions and its orbit will also shrink and circularize due to gravitational radiation. The star may eventually be tidally disrupted, but on an orbit that is much more bound than in the standard scenario. This will lead to a remnant disc of the type analysed by Cannizzo, Lee & Goodman (1990), for which the accretion rate decreases more slowly than in the parabolic scenario:  $\dot{M} \sim t^{-1.2}$  for reasonable opacities. If flare light curves are sampled sufficiently these decays could in principle be distinguished from each other, which would give us new insight into stellar dynamics and the prospects for EMRIs.

Here we present numerical and analytical analyses of binary tidal separation and subsequent tidal disruption of the remaining star. We note that there exist similar but not identical numerical studies. In particular, Gould & Quillen (2003) use a mass for the black hole of  $3.6 \times 10^6 M_{\odot}$  but show results only for the subset that gives captured stars with similar parameters to the observed stars S2-0. Their initial binary distributions are similar to ours, although they do not examine binaries with initial semimajor axis  $< 1$  au and focus on higher masses. Ginsburg & Loeb (2006) address a black hole mass of  $4 \times 10^6 M_{\odot}$  and their binaries are formed of two stars of masses  $3 M_{\odot}$ . They present a few sample orbits of captured stars similar to the S stars, but do not give a detailed distribution. Perets & Gualandris (2010) also focus on  $4 \times 10^6 M_{\odot}$  massive black holes

\*E-mail: Pau.Amaro-Seoane@aei.mpg.de

(MBHs), and find as expected that the captured stars tend to have high eccentricities  $e > 0.97$ , but do not give a periastron distribution for the stars. Madigan, Levin & Hopman (2009) present in their notable work direct-summation  $N$ -body simulations of small discs of stars with semimajor axes of 0.026 and 0.26 pc with  $4 \times 10^6 M_{\odot}$  MBHs, which produced stars with high eccentricities that did not, however, enter the region of greatest interest to us. Hence we have performed new numerical simulations to explore our scenario.

In Section 2 we discuss tidal separations and present our three-body simulations of the process. In Section 3 we use these results as initial conditions and analyse the competition between stellar dynamical processes (which can raise or lower the eccentricity) and gravitational radiation (which shrinks and circularizes the orbit) to determine the mass ranges most likely to lead to moderate eccentricities at the point of disruption. In Section 4 we discuss the tidal process itself, and argue that the small but non-zero residual eccentricities mean that for sufficiently low-mass SMBHs the star will typically be disrupted rather than settling into a phase of steady mass accretion on to the SMBH. We present our conclusions in Section 5.

## 2 BINARY TIDAL SEPARATION

Tidal separation of binaries by SMBHs was first discussed by Hills (1988). He suggested that one member of the binary would be ejected with a velocity of  $> 10^3 \text{ km s}^{-1}$ , a ‘hypervelocity star’; several such objects have now been observed (see Brown et al. 2009 for a discussion of their observed properties). The other member would settle into a fairly tightly bound orbit around the SMBH; see Miller et al. (2005) for a discussion in the context of EMRIs into an SMBH.

To simulate this process we assume a uniform distribution of pericentre distances between 1 and 700 au for the orbit of the binary around a  $10^7 M_{\odot}$  MBH. The initial orbit is also assumed to be parabolic and to have its relative inclination uniformly distributed over a sphere. In total 228 000 numerical simulations were conducted using a generalized three-body code described by Zare (1974) and Aarseth & Zare (1974). This numerical integrator is based on Kustaanheimo–Stiefel regularization of a two-body system, which is described in Kustaanheimo & Stiefel (1965) and Aarseth (2003). The total energy and angular momentum of the system are conserved to a high degree of accuracy and close encounters between bodies do not induce unphysical velocities.

The resulting distribution for the pericentre distance and eccentricity of the captured population, as well as the velocity distribution for the star re-ejected into the stellar system, are shown in Fig. 1 for an initial internal binary eccentricity of  $e_i = 0.4$  and a stellar mass of  $1 M_{\odot}$ . To produce this figure we chose  $10^7$  sets of parameters for fixed eccentricities and drew the semimajor axis of the initial stellar binary from a log-normal distribution between 0.05 and 10 au. This is taken from observations of the period distribution of binaries in local field stars (Duquennoy & Mayor 1991). The mean would be about 0.37 au.

In the figure we show the resulting probabilities, where we plot the probability of finding a captured star with a particular pericentre distance and eccentricity bin given that a binary is scattered to within 700 au of the MBH. The distribution of semimajor axes for captured stars is shown in Fig. 2 for a  $1 M_{\odot}$  star that was taken from an initial stellar binary with eccentricity  $e_i = 0.0, 0.4, 0.7$  or  $0.9$ .

We now discuss the evolution of the orbits of the stars after capture, under the combined influence of two-body relaxation and gravitational radiation.

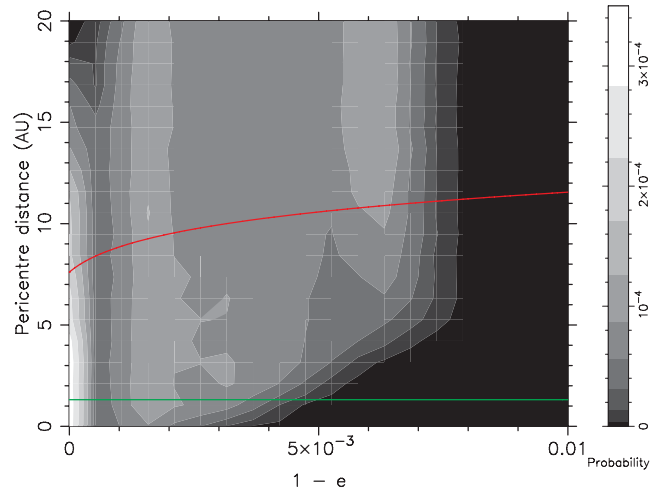


**Figure 1.** Distribution of the pericentre distance and eccentricity of the captured companion at the tidal separation radius for an initial eccentricity of  $e_i = 0.4$  and a stellar mass of  $1 M_{\odot}$ . Other eccentricities do not change significantly the shape of the distribution. The red line indicates the maximum pericentre distance for which the tidal disruption occurs within a Hubble time under the influence of gravitational radiation alone. In the limit  $e \rightarrow 1$ ,  $r_p$  approaches the tidal disruption radius, which we display as a green line, at 1.3 au, although this cannot be seen directly in the figure because we use a resolution of  $\delta e = 10^{-4}$ .

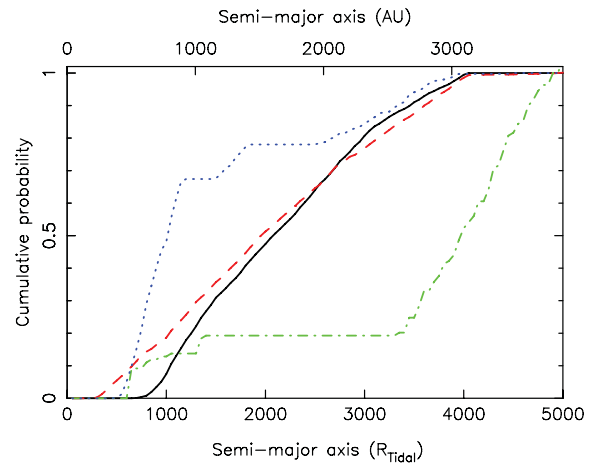


**Figure 2.** Cumulative probability distribution of the semimajor axis of the captured star after the tidal separation of the binary for a  $1 M_{\odot}$  star. The colours denote the initial eccentricity of the binary before being disrupted by the MBH, where black (solid line) denotes  $e_i = 0.0$ , red (dashed line)  $e_i = 0.4$ , green (dot-dashed line)  $e_i = 0.7$  and blue (dotted line)  $e_i = 0.9$ . The probabilities of captures are different in the different eccentricity cases; in particular, the case  $e_i = 0.9$  is easier to capture than the others.

## 3 COMPETITION BETWEEN STELLAR DYNAMICS AND GRAVITATIONAL RADIATION

Suppose that a binary has been tidally separated by a close passage to an SMBH, but that the remaining object is outside the tidal radius (i.e. it is not torn apart yet). Gravitational radiation will circularize the orbit as it shrinks, but dynamical processes can increase the eccentricity. Eventually, the star will move inside the tidal radius and (as we argue in Section 4) will probably be tidally disrupted if the SMBH is of sufficiently low mass.

In this section, we discuss the dynamics subsequent to a tidal separation. We presume that the pericentre of the orbit of the remaining star is outside the tidal radius, so that there is no immediate tidal disruption. The star will then be subjected to two-body interactions that can change the semimajor axis and eccentricity of its orbit. In principle, resonant relaxation (Rauch & Tremaine 1996) could also play a role, in particular due to the high eccentricity the orbit has, since the component of the torque is linearly proportional to eccentricity (Gürkan & Hopman 2007), but for the relevant tight orbits general relativistic pericentre precession essentially eliminates this effect (Merritt et al. 2011). We will therefore focus exclusively on two-body interactions.

The two-body energy relaxation time (during which the semimajor axis of the orbit will be roughly doubled or halved) for a star of mass  $m$  moving against a background of density  $\rho$  and velocity dispersion  $\sigma$  is (Spitzer 1987)

$$t_{\text{en}} \approx \frac{0.3}{\ln \Lambda} \frac{\sigma^3}{G^2 \rho m}. \quad (1)$$

Here  $\ln \Lambda \sim 10$  is the Coulomb logarithm. For our purposes, however, it is not the semimajor axis but the pericentre distance that is important, because this is what determines whether the star enters the tidal region. It is therefore the angular momentum relaxation time that is more relevant. For a nearly circular orbit this time is comparable to the energy relaxation time, but as we saw in Section 2 the initial eccentricity is close to unity in almost all cases. The angular momentum of an orbit scales as  $\sqrt{a(1-e^2)}$ , so an orbit with eccentricity  $e$  has an angular momentum a factor of  $(1-e^2)^{1/2}$  less than a circular orbit with the same semimajor axis. Two-body relaxation is a diffusive process; hence, the expected change in energy or angular momentum after time  $t$  scales as  $t^{1/2}$ . As a result, the angular momentum relaxation time is a factor of  $[(1-e^2)^{1/2}]^2 = 1-e^2$  less than the energy relaxation time:

$$t_{\text{am}} = \frac{0.3}{\ln \Lambda} \frac{\sigma^3}{G^2 \rho m} (1-e^2). \quad (2)$$

For  $e \sim 1$  this is much shorter than the energy relaxation time; hence, we will assume that  $a$  is fixed throughout. We also note that because angular momentum relaxation is a random walk process, the angular momentum could go up or down; if it goes up then nothing interesting happens to the star. Thus we will consider only the case in which the angular momentum and hence the pericentre distance decreases.

To be more quantitative, let us suppose that we have a galactic centre with an SMBH of mass  $M$  with a stellar mass density profile  $\rho(r) = \rho_0(r/r_{\text{infl}})^{-\alpha}$  inside the radius of influence  $r_{\text{infl}} \equiv 2GM/\sigma_0^2$ , where  $\sigma_0$  is the velocity dispersion in the bulge of the galaxy. The radius of influence is by definition the radius inside of which the total stellar mass equals the black hole mass; hence, the normalization is  $\rho_0 = \frac{3-\alpha}{4\pi} \frac{M}{r_{\text{infl}}^3}$ . Suppose we make the simplifying approximation that the velocity dispersion is  $\sigma(r) = \sigma_0(r/r_{\text{infl}})^{-1/2}$  (this scaling is accurate for  $r < r_{\text{infl}}$  but not for  $r \sim r_{\text{infl}}$  because of the mass contribution from stars). Let us assume in addition an  $M-\sigma_0$  relation of the form  $M = 10^8 M_{\odot} (\sigma_0/200 \text{ km s}^{-1})^4$  (Tremaine et al. 2002). Then  $r_{\text{infl}} \approx 3M_7^{1/2}$  pc, where  $M = 10^7 M_7 M_{\odot}$  and

$$t_{\text{am}} \approx 7 \times 10^{11} \text{ yr} (3-\alpha)^{-1} M_7^{5/4} m_0^{-1} (r/r_{\text{infl}})^{\alpha-3/2} (1-e^2) \quad (3)$$

with  $m_0 \equiv m/M_{\odot}$ .  $t_{\text{am}}$  is the time-scale on which two-body processes can raise or lower the pericentre distance significantly. Competing against this is the gravitational radiation time-scale

$$t_{\text{GR}} \approx 3 \times 10^{15} \text{ yr} m_0^{-1} M_7^{-2} \left( \frac{a}{1000 \text{ au}} \right)^4 (1-e^2)^{7/2}. \quad (4)$$

Over a time  $t \approx t_{\text{GR}}$ , the orbit shrinks and circularizes significantly. Setting the two time-scales equal to each other and noting that the pericentre distance is  $r_p = a(1-e)$  gives a critical pericentre distance of

$$r_{p,\text{crit}} \approx 16 \text{ au} (8 \times 10^{-4})^{(2\alpha-3)/5} \times (3-\alpha)^{2/5} M_7^{(8-\alpha)/5} \left( \frac{a}{1000 \text{ au}} \right)^{(2\alpha-6)/5}. \quad (5)$$

Typical values for  $r_{p,\text{crit}}$  can be read directly off of the simulations. For one that can decay faster than a Hubble time, it is  $< 10$  au, and for one that can decay faster than it would be disrupted by two-body relaxation, it is more like 5 au. At a smaller pericentre distance than is given by this expression, gravitational radiation dominates the evolution; conversely, at a larger pericentre distance, two-body relaxation dominates.

At the MBH masses  $\sim 10^7 M_{\odot}$  that we consider, there may or may not be time for the stars to relax dynamically; hence, it is not clear which value of  $\alpha$  to take. If strong mass segregation occurs, then  $\alpha = 2$  is likely (Alexander & Hopman 2009; Preto & Amaro-Seoane 2010; Amaro-Seoane & Preto 2011), but flatter slopes may also be relevant, particularly if there has been scouring by a previous MBH merger and the system has not yet readjusted. For a selection of slopes we find

$$\begin{aligned} r_{p,\text{crit}} &\approx 14 \text{ au} M_7^{13/10} (a/1000 \text{ au})^{-3/5}, & \alpha &= 3/2 \\ r_{p,\text{crit}} &\approx 7 \text{ au} M_7^{5/4} (a/1000 \text{ au})^{-1/2}, & \alpha &= 7/4 \\ r_{p,\text{crit}} &\approx 4 \text{ au} M_7^{6/5} (a/1000 \text{ au})^{-2/5}, & \alpha &= 2. \end{aligned} \quad (6)$$

We will simplify by assuming that gravitational radiation is unimportant until  $r_p = r_{p,\text{crit}}$ , at which point it takes over completely with no further influence from two-body effects. If this is true, then the next question is whether  $r_{p,\text{crit}}$  is greater than the tidal radius. If we focus on main-sequence stars of mass  $m \lesssim M_{\odot}$ , then over a wide range of masses their radii are reasonably fitted by  $R_* \approx 0.85 R_{\odot} (m/M_{\odot})^{2/3}$  (Demircan & Kahraman 1991) and the tidal radius is

$$r_T \approx R_* \left( \frac{3M}{m} \right)^{1/3} \approx 1.3 \text{ au} M_7^{1/3} m_0^{1/3}. \quad (7)$$

Thus we see that stars in this mass range will typically enter the gravitational radiation regime before they are tidally disrupted. Given that the critical pericentre is just a few times the tidal radius, and that many aspects of this calculation are uncertain, it is quite possible that although tidal effects drop off very sharply with distance they could have an impact on the orbit outside  $r_T$ . An exploration of this possibility would require careful hydrodynamic simulations, but for our purposes we will assume that they are not dominant.

Assuming that this is the case, we can compute the eccentricity of the orbit at the point that the pericentre distance equals  $r_T$ , when (as we show in the next section) the star is likely to be tidally disrupted instead of settling into a phase of steady accretion. We calculate the eccentricity by noting that to lowest (quadrupolar) order, pure evolution via gravitational radiation conserves the quantity

$$C = ae^{-12/19} (1-e^2) \left( 1 + \frac{121}{304} e^2 \right)^{-870/2299} \quad (8)$$

(Peters 1964). We saw in Section 2 that the initial eccentricity after tidal separation is nearly unity, so  $1+e \approx 2$ . From our assumptions we also know that  $r_p = a(1-e) = r_{p,\text{crit}}$ . Finally, if we assume that at the tidal radius the eccentricity is  $e_T \ll 1$ , so that  $a_T \approx r_T$ , we get

$$\begin{aligned} a_T e_T^{-12/19} &\approx 1.8 r_{p,\text{crit}} \\ e_T &\approx 0.4 \left( \frac{r_{p,\text{crit}}}{r_T} \right)^{-19/12}. \end{aligned} \quad (9)$$

For our three slopes the eccentricity at the tidal radius is thus

$$\begin{aligned} e_T &\approx 0.01 M_7^{-551/360} m_0^{19/36} (a/1000 \text{ au})^{19/20}, & \alpha = 3/2 \\ e_T &\approx 0.03 M_7^{-209/144} m_0^{19/36} (a/1000 \text{ au})^{19/24}, & \alpha = 7/4 \\ e_T &\approx 0.07 M_7^{-247/180} m_0^{19/36} (a/1000 \text{ au})^{19/30}, & \alpha = 2. \end{aligned} \quad (10)$$

We now explore the consequences of the star sinking inside the tidal radius with this eccentricity, and argue that tidal disruption is the most likely outcome if the SMBH has sufficiently low mass. We then demonstrate that tidal disruption with a small eccentricity leads to a different light curve than the more commonly considered tidal disruption of a star on a parabolic orbit.

#### 4 HYDRODYNAMICS NEAR AND INSIDE THE TIDAL RADIUS

Suppose that the star sinks gradually under the influence of gravitational radiation towards the tidal radius. The tidal stresses increase as  $\sim (R_*/r)^6$ , where  $R_*$  is the stellar radius and  $r$  is the distance from the SMBH. Therefore, the star will be flexed and distorted, and internal modes will be excited as it sinks (for a recent discussion and simple model of this complicated process, see Ogilvie 2009). If the energy from these modes could be dissipated, then the orbit would undergo tidal circularization and might end up in a stable mass transfer state. However, the energy that must be dissipated is significantly larger than the binding energy of the star. To see this, note that at the tidal radius  $r_T$ , we have  $r_T = (3M/m)^{1/3} R_*$ . The binding energy of the star is  $E_* \approx Gm^2/R_*$ . The binding energy of the orbit is  $E_{\text{orb}} \approx GMm/r_T$ . Circularization of an orbit with eccentricity  $e$  at constant angular momentum releases an energy  $e^2 E_{\text{orb}}$ , so the ratio of released energy to stellar binding energy is

$$e^2 \frac{E_{\text{orb}}}{E_*} \approx e^2 \left( \frac{M}{m} \right) \left( \frac{R_*}{r_T} \right) \approx 3^{-1/3} e^2 \left( \frac{M}{m} \right)^{2/3}. \quad (11)$$

If  $M \sim 10^7 m$ , the ratio is therefore  $\sim 3 \times 10^4 e^2$ . From the previous section we found  $e \sim 0.01\text{--}0.07$  for  $M = 10^7 M_\odot$ , so the energy required to circularize the orbit would be  $\sim 3\text{--}150$  times the binding energy of the star. If this energy could be released slowly, this would cause no problems (note for comparison that in its lifetime the Sun will radiate a few hundred times its binding energy). However, the thermal (Kelvin–Helmholtz) time for solar-type stars is a few tens of millions of years, much longer than the inspiral time in our case and thus the tidal stresses will build up more rapidly than their mode energy can be radiated.

The competition is therefore between the time needed for gravitational radiation to move the star into the tidal radius (where mass transfer will ensue) and the time needed for circularization due to tidal dissipation to deposit stellar binding energy into the star and thus, presumably, to tidally disrupt the star. Note that Alexander & Morris (2003) discussed how tidal energy could produce ‘squeezars’ with a different appearance from normal stars, without destroying the stars if the pericentre distance is sufficiently large. Here we are interested in the conditions for tidal destruction.

To evaluate this we adapt the expressions from Leconte et al. (2010) for the energy deposition rate of tidal dissipation in a planet due to its eccentric orbit around a star. They find

$$\dot{E}_{\text{tides}} = 2K_p \left| N_a(e) - \frac{N^2(e)}{\Omega(e)} \right|, \quad (12)$$

where

$$N(e) = \frac{1 + \frac{15}{2}e^2 + \frac{45}{8}e^4 + \frac{5}{16}e^6}{(1 - e^2)^6}, \quad (13)$$

$$N_a(e) = \frac{1 + \frac{31}{2}e^2 + \frac{255}{8}e^4 + \frac{185}{16}e^6 + \frac{25}{64}e^8}{(1 - e^2)^{15/2}}, \quad (14)$$

$$\Omega(e) = \frac{1 + \frac{3}{2}e^2 + \frac{1}{8}e^4}{(1 - e^2)^5} \quad (15)$$

and

$$K_p \approx \frac{9}{4} Q^{-1} \left( \frac{Gm^2}{R_*} \right) \left( \frac{M}{m} \right)^2 \left( \frac{R_*}{a} \right)^6 \left( \frac{GM}{a^3} \right)^{1/2}. \quad (16)$$

In the last equation  $Q$  is the quality factor of the star, a standard parametrization of the rate of tidal effects on to the star. The magnitude of  $Q$  is notoriously uncertain; values of  $Q = 10^{5-6}$  are commonly used (see, e.g., Miller, Fortney & Jackson 2009 for a recent example). If we use the expression  $a_T = (3M/m)^{1/3} R_*$  for the tidal radius, the last expression reduces to

$$K_p \approx \frac{1}{4} Q^{-1} \left( \frac{Gm^2}{R_*} \right) \left( \frac{a}{a_T} \right)^{-6} \left( \frac{GM}{a^3} \right)^{1/2}. \quad (17)$$

In the limit  $e < 1$  we find  $N_a(e) \approx 1 + 23e^2$ ,  $N^2(e) \approx 1 + 27e^2$  and  $\Omega(e) \approx 1 + \frac{15}{2}e^2$ . Thus

$$\dot{E}_{\text{tides}} \approx \frac{7}{4} Q^{-1} e^2 \left( \frac{Gm^2}{R_*} \right) \left( \frac{a}{a_T} \right)^{-6} \left( \frac{GM}{a^3} \right)^{1/2}. \quad (18)$$

Thus the time needed to circularize the available energy  $\sim e^2 (M/3m)^{2/3} (Gm^2/R_*)$  at  $a = a_T$  is

$$\begin{aligned} T_{\text{circ,tide}} &\approx e^2 (M/3m)^{1/3} (Gm^2/R_*) \\ &\quad \times \left[ (7/4) Q^{-1} e^2 (Gm^2/R_*) (GM/a^3)^{1/2} \right]^{-1} \\ &= 3 \times 10^7 \text{ s } Q M_7^{2/3} m_0^{-1/6}, \end{aligned} \quad (19)$$

where in the second line we have substituted  $R_* = 0.85 R_\odot m_0^{2/3}$  and  $a_T = (3M/m) R_*$ . The circularization time from gravitational radiation alone, at  $e \ll 1$ , is

$$\begin{aligned} T_{\text{circ,GW}} &\approx (15/304) c^5 a^4 / (G^3 \mu M^2) \\ &\approx 6 \times 10^{11} \text{ s } M_7^{-2/3} m_0^{1/3} \end{aligned} \quad (20)$$

(Peters 1964), where in the last line we again substituted in  $a = a_T$ . Thus  $T_{\text{circ,GW}}/T_{\text{circ,tide}} \approx 2 \times 10^4 Q^{-1} M_7^{-4/3} m_0^{1/2}$ , which for  $Q \sim 10^{5-6}$  is typically less than unity; hence, only a fraction  $T_{\text{circ,GW}}/T_{\text{circ,tide}}$  of the circularization energy will go into tidal heating. Note, however, that for lower masses the eccentricity at the tidal radius is larger (scaling roughly as  $M^{-3/2}$  for our three power laws) and that the ratio of the circularization energy to the internal binding energy scales as  $e^2$ , meaning that the total energy dissipated tidally scales as  $\sim M^{-4}$ , approximately. Thus even for  $Q = 10^6$ , several times the stellar binding energy will be dissipated for  $M < 3 \times 10^6 M_\odot$ .

If instead the SMBH mass is large, so that gravitational wave circularization dominates tidal circularization, we expect that the star will settle into a period of steady mass transfer. The rate would be such that it balances the inward movement due to gravitational radiation, i.e. the characteristic time would be of the order of the gravitational radiation time. For our typical values, this is roughly  $10^5$  yr, implying a rate of  $\sim 10^{-5} M_\odot \text{ yr}^{-1}$ . Even if the luminosity is produced with an efficiency of 10 per cent, this would produce a luminosity of only  $\sim 10^{41} \text{ erg s}^{-1}$ , weak enough and steady enough that it would not be distinguishable from a standard low-luminosity AGN. We therefore focus on the possibility that the star is tidally disrupted and that its debris is subsequently accreted by the SMBH.

If a star is disrupted from a low-eccentricity orbit the evolution of its tidal debris proceeds differently than if it is disrupted from a parabolic orbit. To see this, note that in the original argument of Rees (1988) it was demonstrated that the spread in the binding energy of the debris is comparable to the range in orbital binding energy from one side of the star to the other. If  $m/M \sim 10^{-7}$ , therefore, the fractional spread is  $\sim (m/M)^{1/3} \sim 10^{-2}$ . As a result, if an orbit with a pericentre  $r \sim r_T$  has an eccentricity  $e \gtrsim 0.99$ , the debris semi-uniformly samples binding energies from zero to the binding energy of the original stellar centre of mass. The assumption of exactly uniform sampling (equal mass for equal range in binding energy) leads to a mass accretion rate that scales with time  $t$  as  $t^{-5/3}$ ; this law is more generally obtained at late times even for more realistic assumptions about stellar structure (e.g. Lodato et al. 2009). In contrast, if the spread in debris energies is much less than the average binding energy (corresponding to  $e \ll 0.99$  in our example), then to lowest order the debris moves in a thin stream that intersects itself and settles within a few orbits into a remnant disc.

Such discs were studied by Cannizzo et al. (1990), who found that for plausible opacities the accretion rate would decay more gradually, e.g.  $\dot{M} \propto t^{-1.2}$  for Thomson scattering. Moreover, because the debris would all be bound to the SMBH (unlike for the parabolic case, where roughly half of the stellar mass escapes to infinity), the accretion rate could be quite substantial for comparatively low-mass SMBHs. For Thomson scattering, the expressions from Cannizzo et al. (1990) lead to

$$\dot{M} = 2 \times 10^{23} \text{ g s}^{-1} \left( \frac{\alpha}{0.1} \right)^{4/3} \bar{\rho}^{7/9} M_7^{-10/9} \left( \frac{\Delta M}{M_\odot} \right)^{5/3}. \quad (21)$$

Here  $\bar{\rho}$  is the average density of the star in units of  $\text{g cm}^{-3}$ ,  $\Delta M$  is the mass of the remnant disc (which will initially be the mass of the star) and  $\alpha$  is the Shakura & Sunyaev (1973) viscosity parameter. For  $M_7 \lesssim 1$  this therefore has the possibility of shining at luminosities that are a significant fraction of the Eddington luminosity  $L_E = 1.3 \times 10^{45} M_7 \text{ erg s}^{-1}$  assuming an efficiency  $L/\dot{M}c^2 = 0.1$ .

As pointed out to us by Phinney (personal communication), depending on the very uncertain details of how tidal energy is deposited, it is possible that there will be a gravitational wave signature that attends the electromagnetic signature of disruption. In particular, it is not well established whether the tidal energy is deposited uniformly in the volume of the star or primarily where most of the matter is (both of which would lead to full disruption) or primarily in the envelope. If the last occurs, then the envelope would be stripped and lead to significant accretion with the characteristic decay discussed above, but the dense core would survive and could spiral in further. This would lead to a coincident gravitational wave signal that could be detected with the proposed *LISA* if the source is close enough (Freitag 2003).

## 5 CONCLUSIONS

In his work, Hopman (2009) estimates that for a galactic nucleus such as ours, the tidal separation rate of binaries which start far away from the MBH is  $\Gamma_{\text{tid sep}}^{\text{GC}} \sim 7 \times 10^{-7} (f_b)^{\text{GC}}/0.05 \text{ yr}^{-1}$ , where ‘GC’ stands for Galactic Center and  $f_b$  is the fraction of stars in binaries. Fig. 6 of Hopman (2009) shows that the rate increases when we go to higher energies, because the loss-cone is depleted, allowing more binaries to ‘survive’ in their way to the GC. Yu & Tremaine (2003) estimate that the number is enhanced by an order of magnitude by binaries *not* bound to the MBH. More remarkably, the event rates can be at least temporarily enhanced by *many orders*

*of magnitude* if one considers the role of massive perturbers, such as giant molecular clouds or intermediate mass black holes, which can accelerate relaxation by orders of magnitude as compared to two-body stellar relaxation (Perets, Hopman & Alexander 2007). Another important potential boosting effect is the possibility that the potential is triaxial and not spherically symmetric (Poon & Merritt 2002, 2004; Merritt & Poon 2004). Taking these effects into account, we assume  $\Gamma_{\text{tid sep}}^{\text{GC}} \sim 10^{-5} (f_b)^{\text{GC}}/0.05 \text{ yr}^{-1}$ . The fraction of main-sequence stars that will eventually spiral into the SMBH after tidal separation is at least a few per cent, so a plausible estimate of the total event rate for tidal disruptions of a single star originated by a separated binary in a Hubble time is  $\Gamma^{\text{GC}} \sim 10^{-7} (f_b)^{\text{GC}}/0.05 \text{ yr}^{-1}$ , and it could be higher. This rate is probably a subset of the rate at which single stars are likely to encounter SMBHs on parabolic orbits (see Amaro-Seoane et al. 2007, for a discussion of such EMRIs). It is therefore possible that events with the  $L \propto t^{-1.2}$  decay characteristic of low-eccentricity disruption may have rates smaller than or similar to events with the  $L \propto t^{-5/3}$  decay that is expected to be signatures of disruption of single stars in galactic nuclei and that is consistent with the initial decay of the recent *Swift* event Sw 1644+57 (Bloom et al. 2011).

## ACKNOWLEDGMENTS

The authors thank the referee for several useful suggestions. PAS thanks Maite Miranda Cascales for the sudden and unexpected two hours’ break in a small Berlin bar on the way home, which led to the first calculations of the paper accompanied by a little bottle of weinbrand. He is indebted to José María Ibáñez and his group for the invitation to visit the Departament d’Astronomia i Astrofísica de la Universitat de València, as well as to Jorge Cuadra for his visit at the Universidad Católica de Chile, where part of this work was done. MCM thanks Sterl Phinney for valuable discussions. MCM was supported in part by NASA grants NNX08AH29G and NNX12AG29G. PAS and MCM are indebted to the Aspen Center for Physics and the organizers of the summer 2011 meeting. GFK thanks the AEI for a visit in 2011.

## REFERENCES

- Aarseth S. J., 2003, *Gravitational N-Body Simulations*. Cambridge Univ. Press, Cambridge
- Aarseth S. J., Zare K., 1974, *Celest. Mech.*, 10, 185
- Alexander T., Hopman C., 2009, *ApJ*, 697, 1861
- Alexander T., Morris M., 2003, *ApJ*, 590, L25
- Amaro-Seoane P., Preto M., 2011, *Class. Quantum Grav.*, 28, 094017
- Amaro-Seoane P., Gair J. R., Freitag M., Miller M. C., Mandel I., Cutler C. J., Babak S., 2007, *Class. Quantum Grav.*, 24, 113
- Amaro-Seoane P. et al., 2012, preprint (arXiv:e-prints)
- Bloom J. S. et al., 2011, *Sci*, 333, 203
- Brown W. R., Geller M. J., Kenyon S. J., Bromley B. C., 2009, *ApJ*, 690, L69
- Cannizzo J. K., Lee H. M., Goodman J., 1990, *ApJ*, 351, 38
- Demircan O., Kahraman G., 1991, *Ap&SS*, 181, 313
- Dogiel V. A. et al., 2009, *PASJ*, 61, 1099
- Donley J. L., Brandt W. N., Eracleous M., Boller T., 2002, *AJ*, 124, 1308
- Duquennoy A., Mayor M., 1991, *A&A*, 248, 485
- Freitag M., 2003, *ApJ*, 583, L21
- Gezari S. et al., 2009, *ApJ*, 698, 1367
- Ginsburg I., Loeb A., 2006, *MNRAS*, 368, 221
- Gould A., Quillen A. C., 2003, *ApJ*, 592, 935
- Gürkan M. A., Hopman C., 2007, *MNRAS*, 379, 1083
- Hills J. G., 1988, *Nat*, 331, 687
- Hopman C., 2009, *ApJ*, 700, 1933

- Kustaanheimo P. E., Stiefel E. L., 1965, *J. Reine Angew. Math.*, 218, 204  
Leconte J., Chabrier G., Baraffe I., Levrard B., 2010, *A&A*, 516, A64  
Lodato G., King A. R., Pringle J. E., 2009, *MNRAS*, 392, 332  
Madigan A.-M., Levin Y., Hopman C., 2009, *ApJ*, 697, L44  
Merritt D., Poon M. Y., 2004, *ApJ*, 606, 788  
Merritt D., Alexander T., Mikkola S., Will C. M., 2011, *Phys. Rev. D.*, 84, 044024  
Miller M. C., Freitag M., Hamilton D. P., Lauburg V. M., 2005, *ApJ*, 631, L117  
Miller N., Fortney J. J., Jackson B., 2009, *ApJ*, 702, 1413  
Ogilvie G. I., 2009, *MNRAS*, 396, 794  
Perets H. B., Gualandris A., 2010, *ApJ*, 719, 220  
Perets H. B., Hopman C., Alexander T., 2007, *ApJ*, 656, 709  
Peters P. C., 1964, *Phys. Rev.*, 136, 1224  
Poon M. Y., Merritt D., 2002, *ApJ*, 568, L89  
Poon M. Y., Merritt D., 2004, *ApJ*, 606, 774  
Preto M., Amaro-Seoane P., 2010, *ApJ*, 708, L42  
Rauch K. P., Tremaine S., 1996, *New Astron.*, 1, 149  
Rees M. J., 1988, *Nat*, 333, 523  
Shakura N. I., Sunyaev R. A., 1973, *A&A*, 24, 337  
Spitzer L., 1987, *Dynamical Evolution of Globular Clusters*. Princeton Univ. Press, Princeton, NJ, p. 191  
Tremaine S. et al., 2002, *ApJ*, 574, 740  
Wang J., Merritt D., 2004, *ApJ*, 600, 149  
Yu Q., Tremaine S., 2003, *ApJ*, 599, 1129  
Zare K., 1974, *Celest. Mech.*, 10, 207

This paper has been typeset from a  $\text{\TeX}/\text{\LaTeX}$  file prepared by the author.